



ELSEVIER

Journal of Electron Spectroscopy and Related Phenomena 94 (1998) 243–252

JOURNAL OF
ELECTRON SPECTROSCOPY
and Related Phenomena

Isomeric sensitivity of the C 1s spectra of xylenes

I.G. Eustatiu, B. Huo, S.G. Urquhart¹, A.P. Hitchcock**Department of Chemistry, McMaster University, Hamilton, L8S 4M1, Canada*

Received 1 December 1997; revised 10 March 1998; accepted 10 March 1998

Abstract

Oscillator strengths for C 1s inner-shell excitation of the isomeric xylenes (*ortho*-, *meta*- and *para*-) have been derived from electron energy loss spectra recorded under scattering conditions dominated by electric dipole transitions. The lineshape of the C 1s $\rightarrow \pi^*$ transition is found to be dependent on the substitution pattern, with *para*-xylene exhibiting two components, *ortho*-xylene a single asymmetric peak, and *meta*-xylene a single symmetric peak at an instrumental resolution of 0.35 eV. Improved virtual orbital ab initio calculations were carried out on all three species, providing spectral shapes in reasonable agreement with experiment. The calculations indicate that the transition responsible for the splitting which is observed only in the C 1s spectrum of *para*-xylene is associated with the methyl-substituted ring carbons, for which there is a somewhat larger chemical shift in the *para* relative to the *ortho*- or *meta*-isomers. These results are compared to other recent studies of C 1s spectroscopy of di-substituted benzenes (dimethylphthalates and nitroanilines) in order to investigate trends in the sensitivity of C 1s spectroscopy to isomeric substitution patterns. © 1998 Elsevier Science B.V. All rights reserved

Keywords: EELS; C 1s excitation spectra; Xylenes; Isomeric effects; Ab initio calculations

1. Introduction

The electronic structure of the xylene isomers has been investigated by a number of different spectroscopic techniques. Valence-shell electron energy-loss spectroscopy [1] has been used to study triplet states in the 4–8 eV energy region. Phosphorescence [2] and optical absorption studies [3] have been used to probe valence electronic excitation. Photoelectron spectroscopy [4] has mapped the energies of the occupied valence levels. When two hydrogen atoms of benzene are substituted with methyl groups, as in the xylenes, the symmetry of the molecule is lowered, and the degenerate π orbitals of benzene are split into

non-degenerate components. The consequences of this descent-in-symmetry splitting are an interesting aspect of xylene spectroscopy. Uno et al. [5] studied the charge transfer spectra of *meta*-dimethyl benzene (*meta*-xylene) and other *meta*-disubstituted benzenes (dichloro-benzene and dibromo-benzene) to determine how the degenerate benzene e_{1g} HOMO splits into a_2 and b_2 orbitals when substituents are introduced in the *m*-position. They used both semiempirical and ab initio calculations (at the STO-3G level) of many *meta*-disubstituted benzenes to determine that the HOMO is invariably either the a_2 - or b_2 -like π orbital, but which one is the HOMO depends on the substituent. Similar studies on *para*-disubstituted benzenes [6] showed that the HOMO donor orbital of *para*-substituted benzenes is always the b_2 component.

Here, we report the first studies of the *inner-shell* excitation spectra of xylenes. The focus of our study is

* To whom correspondence should be addressed

¹ Present address: Department of Physics, North Carolina State University, Raleigh, NC, USA.

the isomeric dependence of the C 1s spectrum, in particular the shape of the lowest energy π^* band. This provides complementary information about the effect of symmetry reduction on the π system since there is often a close relationship between the symmetry splittings of the π and π^* levels. Our study was motivated by recent investigations of the C 1s spectra of isomeric dimethylphthalates (1,2-DMP, 1,3-DMP and 1,4-DMP) [7] and isomeric nitroanilines (*ortho*-, *meta*- and *para*-) [8]. In each of these series the shape of the C 1s $\rightarrow \pi^*$ spectral feature was found to be dependent on the substitution. In the dimethylphthalates the lowest energy C 1s $\rightarrow \pi^*$ band in 1,4-DMP has two components, whereas the 1,3- and 1,2-DMP isomers exhibit only single peaks. According to both high-quality ab initio and semi-empirical calculations of the C 1s spectra of the three DMP isomers, the second peak in 1,4-DMP is the C 1s $\rightarrow \pi^*(a_2)$ transition, which the calculation predicts has negligible intensity in 1,2-DMP and 1,3-DMP [7]. In the isomeric nitroanilines [8], a similar experimental trend was observed, with the main C 1s $\rightarrow \pi_{\text{ring}}^*$ feature of *para*-nitroaniline exhibiting a distinct high-energy shoulder which is not present in the other two isomers. However, the C 1s spectra of nitroanilines are complicated because of strong mixing of π_{NO}^* and $\pi_{\text{C=C}}^*$ levels and thus an unambiguous determination of the isomeric dependence of the C 1s $\rightarrow \pi_{\text{C=C}}^*$ band shape could not be obtained. The results to date on disubstituted benzenes suggest that a splitting of the main C 1s $\rightarrow \pi^*$ signal may be a characteristic marker of *para* substitution. However, both the dimethylphthalate and nitroaniline cases are complicated by other perturbations, such as ligand-ring delocalization, which are likely also dependent on the pattern of isomeric substitution. In order to examine the effect of ring substitution pattern with a minimum of other effects, we have turned to the xylenes to make an experimental test of this hypothesis. In addition to measuring the C 1s spectra of the three xylene isomers at 0.7 and 0.35 eV resolution, we have used ab initio calculations based on Kosugi's GSCF3 methodology [9,10] to provide a theoretical base for our spectral interpretations.

2. Experiment

The spectra were measured using two different

electron energy-loss spectrometers. One [11] uses an unmonochromated incident electron beam, a final electron energy of 2.5 keV, a collision cell, and was operated with a resolution of 0.7 eV. The second instrument is a variable impact energy, variable-angle spectrometer that has improved resolution, selected as 0.35 eV for this work. After monochromatization and acceleration to the chosen impact energy, the electron beam is scattered by the gas in an effusive jet. Electrons inelastically scattered at a mechanically determined scattering angle are retarded, and energy analysed using a hemispherical electron energy analyser. The high resolution spectra were recorded using a residual electron energy of 1300 eV and at a scattering angle of 4°. Both the 290.74 eV π^* peak in CO₂ and 287.40 eV π^* peak in CO were used for calibration. Freeze–pump–thaw iterations were performed on the samples, which were otherwise used as received from the commercial supplier (Aldrich, 99% purity). The measured spectra were background subtracted to remove the underlying valence ionisation continuum, subjected to a kinematic correction, and then converted to an absolute oscillator strength intensity scale using a method described elsewhere [12].

3. Calculations

The energies and oscillator strengths for C 1s core-excitations in each xylene isomer were obtained by ab initio Δ SCF (self-consistent field) calculations using GSCF3 [9] with explicit consideration of the core hole [10] in a localised core hole picture. The basis set is the (63/5) contracted [13] Gaussian-type extended basis set for carbon and (5) for hydrogen. A contraction scheme of (411121/3111/1*) was used for the carbon atom with the localised core hole, (621/41) for the other carbon atoms and (41) for hydrogen. The core-excitation energies and intensities were obtained with the improved virtual orbital (IVO) method [14]. The relaxed Hartree–Fock (HF) potential is essential to accurately reproduce the large electronic reorganisation that occurs upon inner-shell hole creation; therefore, the IVO method based on the relaxed HP potential is superior to the method using the ground-state orbitals. This approach has been shown to be quite accurate in predicting term values and intensities of core excitations [15,16].

Table 1
Bond lengths and bond angles used for computations^a, compared to experimental values (*ortho*, *meta*)^b

Bond	Bond length (Å)			Angle	Bond angle (°)		
	<i>ortho</i> -xylene	<i>meta</i> -xylene	<i>para</i> -xylene		<i>ortho</i> -xylene	<i>meta</i> -xylene	<i>para</i> -xylene
(C–C) _{ring}	1.400 (1.394, 1.398, 1.414)	1.400	1.400 (1.405)	(C–C–C) _{ring}	120 (119–121)	120	120 (121)
(C–Me)	1.509 (1.509)	1.509	1.512 (1.512)	(C–(CR)–C)	120 (120)	120	120 (117)
(C–H) _{ring}	1.09 (1.072)	1.09	1.09 (1.103)	(C–C)–Me	120 (120)	120	120 (121)
(C–H) _{methyl}	1.09 (—)	1.09	1.09 (1.113)	(C–C–H) _{ring}	120 (120)	120	120 (121)
				C–C _{Me} –H	110 (111)	110	110 (110)

^a The computational geometry was derived by ab initio energy minimization, with symmetry assumptions as described in the text.

^b The experimental geometry of *ortho*-xylene was determined by microwave spectroscopy while that of *para*-xylene was determined from electron diffraction [18].

SPARTAN [17] was used to generate the molecular geometries used for the high-level calculations. We assumed that all C–C bonds in the phenyl ring are the same length and that all C–C–C and H–C–C

bond angles are 120°. Table 1 gives the geometries used with comparison to gas phase experimental geometries for *ortho*- and *para*-xylene [18]. For each species, the calculated IVO term values and oscillator

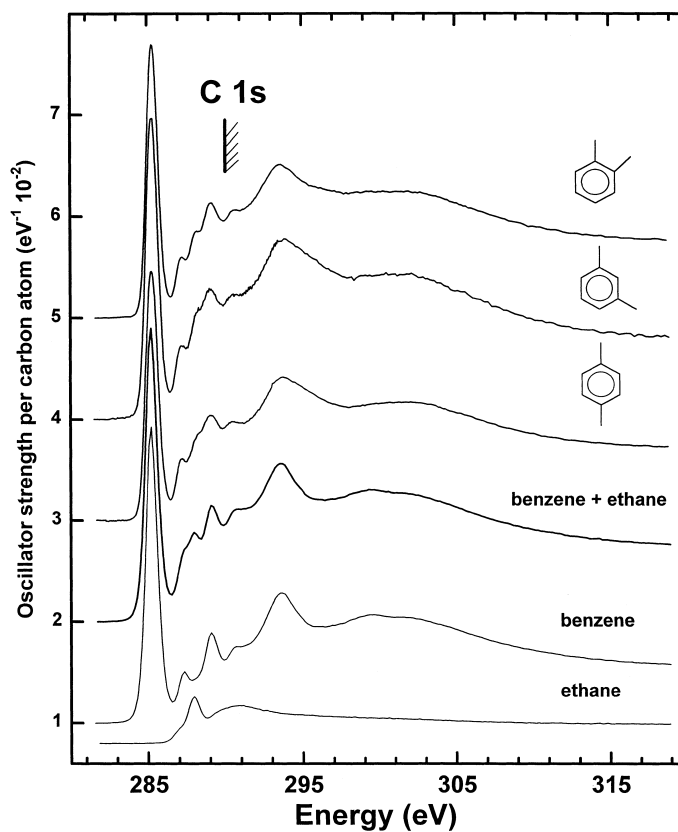


Fig. 1. C 1s oscillator strengths (per carbon atom) derived from electron energy-loss spectra of *para*-, *meta*- and *ortho*-xylene in the C 1s region, recorded with 2500 eV final electron energy, a scattering angle of $\sim 2^\circ$, and a resolution of 0.7 eV FWHM. Offsets are used for clarity. The spectra of benzene [19] and ethane [20], as well as a 0.75:0.25 weighted sum are also plotted.

strengths for the C 1s excitations were combined with the calculated absolute C 1s ionisation energy to generate a predicted C 1s spectrum on an absolute energy scale. In order to facilitate comparison with experiment, the calculated results were broadened using Gaussian linewidths of: 5 eV full width at half maximum (FWHM) for orbitals of eigenvalue (ϵ) above +5 eV; 2 eV for $+2 < \epsilon < +5$; 1 eV for $0 < \epsilon < +2$ and 0.3 eV for bound states.

4. Results

Fig. 1 presents long-range C 1s oscillator strength spectra recorded using the unmonochromated electron spectrometer with an energy resolution of 0.7 eV FWHM. Energies, estimated term values and proposed assignments of spectral features are listed in Table 2. At this resolution the spectra of all three isomers are very similar. In addition to the spectra of the xylenes, Fig. 1 also plots the C 1s spectra of benzene [19] and ethane [20] along with that of a spectral simulation consisting of a weighted sum of the spectra of benzene and ethane. Overall the xylene

spectra are quite similar to that of the spectral simulation, although the 287–292 eV region is more congested in the xylenes and the strong continuum resonance at 294 eV has a distinct asymmetry on the high energy side, which is not present in the simulation, or the spectrum of benzene.

Careful examination of the spectra recorded with the limited energy resolution of the unmonochromated spectrometer indicated that the main π^* peak in *para*-xylene is wider than that of the other two isomers. In order to investigate this further, we used the spectrometer with a monochromated electron beam to record higher resolution spectra (0.35 eV fwhm) over a short energy range. Note that the long-range spectra acquired with the low resolution spectrometer are essential for establishing accurate oscillator strength scales. At present, the acquisition time for a 40 eV wide spectrum would be unacceptably long with the monochromated instrument. Fig. 2 compares the discrete region of the C 1s spectra of the three isomers, recorded with both instruments. More spectral detail is revealed at higher resolution. These spectra are a complicated overlap of transitions in which electrons in four or more core levels which

Table 2

Experimental energies (eV), term values (eV) and proposed assignments for features in the C 1s spectra of *ortho*-, *meta*- and *para*-xylene

<i>ortho</i> -xylene			<i>meta</i> -xylene			<i>para</i> -xylene			Assignment (final level)					
Energy (eV)	TV (eV)			Energy (eV)	TV (eV)			Energy (eV)	TV (eV)			C-H	C-R	Me
	T _{C-H}	T _{C-R}	T _{Me}		T _{C-H}	T _{C-R}	T _{Me}		T _{C-H}	T _{C-R}	T _{Me}			
285.38(8) ^a	4.9			285.4 ^b	4.9			285.15(6)	5.1			1 π^*		
285.8		5.1		(285.4)			(5.5)	285.40(6) ^c		5.5			1 π^*	
287.1	3.2			287.1	3.2			287.1	3.2			3s		
287.4	2.9	3.5		287.4	2.9	3.5		287.3	3.0	3.6		3p	3s	
288.1			2.0	288.2			1.9	288.0			2.1			$\pi^*/\text{C-H}$
								288.3			1.8			$\pi^*/\text{C-H}$
289.0	1.3			288.9	1.4			288.9	1.4			2 π^*		
289.3		1.6		289.3		1.6		289.2		1.7			2 π^*	
290.1				290.1				290.1						IP ^d
290.3				290.3				290.3				IP ^d		
290.9				290.9				290.9				IP ^d		
290.7 (3)				290.7 (3)				290.5 (3)						
293.6 (3)				293.8 (3)				293.8 (3)					— 1 σ^* —	
300.9 (3)				300.9 (3)				300.7 (3)					— 2 σ^* —	

^a Calibration: $-5.35(4)$ eV relative to π^* of CO₂ (290.74(4) eV) and $-2.00(2)$ eV relative to π^* of CO (287.40(2) eV).

^b Calibration: $-5.40(4)$ eV relative to π^* of CO₂ and $-2.00(2)$ eV relative to π^* of CO.

^c Calibration: $-5.38(4)$ eV relative to π^* of CO₂ and $-2.00(2)$ eV relative to π^* of CO.

^d The IPs were estimated from those of toluene [21]: C₆H₅CH₃, 290.1 eV; C₆H₅CH₃, (C-H) 290.3 eV; C₆H₅CH₃, (C-R) 290.9 eV.

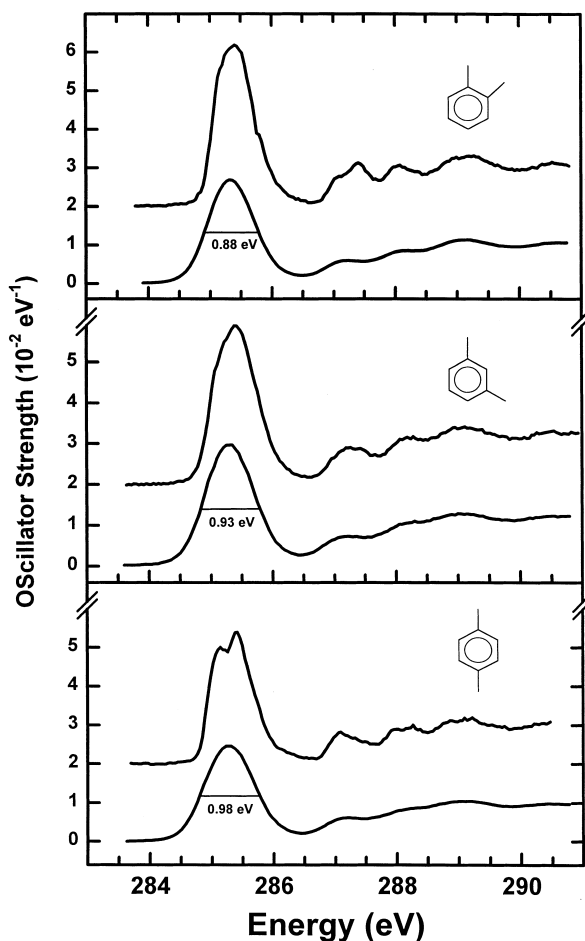


Fig. 2. C 1s oscillator strengths derived from electron energy-loss spectra of *para*-, *meta*- and *ortho*-xylene in the C 1s region recorded with 1300 eV final electron energy, a scattering angle of 4° and a resolution of 0.35 eV FWHM. The corresponding regions of the low-resolution spectra are also plotted for comparison.

are estimated to be distributed over ~ 0.8 eV are excited to a set of split π^* levels, with the a_2/b_2 splitting likely dependent on the location of the core hole. Thus it is noteworthy that more spectral detail was revealed as the resolution was increased.

A split π^* peak was found in *para*-xylene, with the maxima of these features occurring at 285.1 and 285.4 eV. In contrast, the spectrum of *meta*-xylene exhibits a single nearly symmetric peak, while *ortho*-xylene has a more asymmetric single peak, with evidence of a shoulder on the high-energy side. In addition to the enhanced resolution in the main π^* region, these spectra also show more detail in the 286–290 eV region. This region contains structures

arising from C 1s excitation to Rydberg and the higher-energy $2\pi^*$ level (correlating with b_{2g} in benzene). Relative to C_6H_6 there is an additional signal at 288 eV in the xylenes which has two components in the *para*- but only one component in the *ortho*- and *meta*-isomers.

Fig. 3 presents the calculated oscillator strength spectra of *ortho*-, *meta*- and *para*-xylene. In each species the total spectrum is the sum of a number of components, corresponding to the chemically inequivalent carbon atoms in each molecule (carbon atom numbering is given in Fig. 3). Calculations were made for each unique site and the sum was generated, taking into account the site degeneracy.

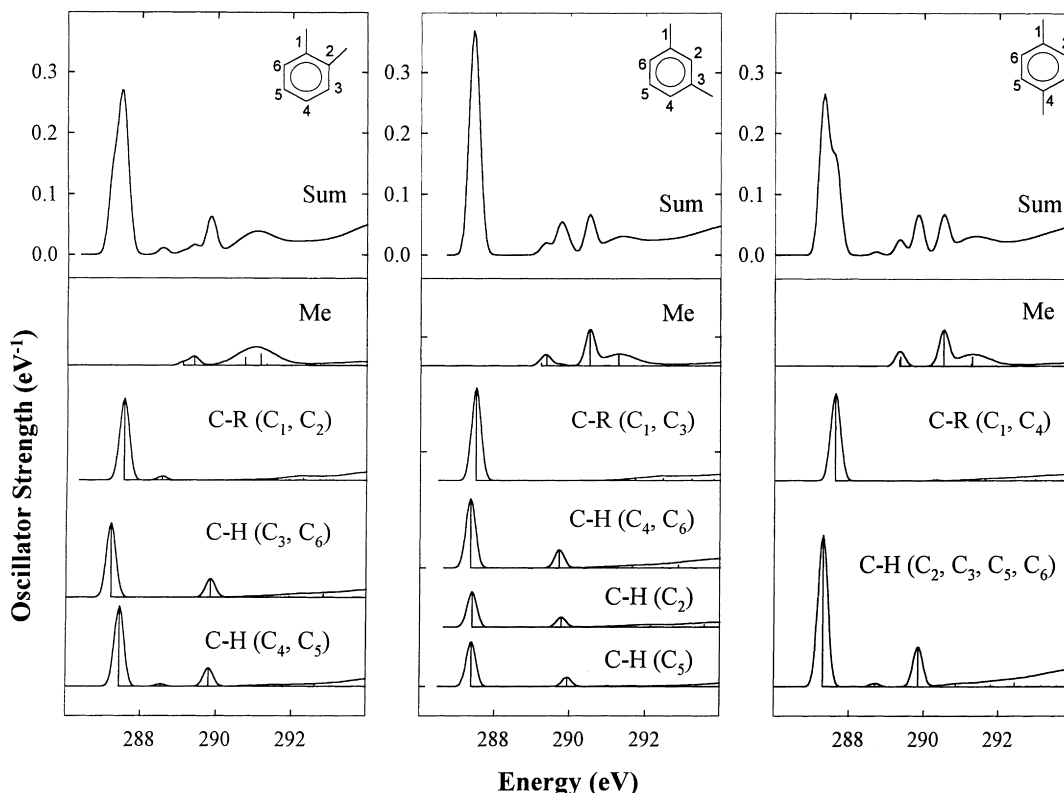


Fig. 3. Spectra simulated from intensity and excitation energies generated from the results of ab initio GSCF3 calculations for C 1s excited *para*-, *meta*- and *ortho*-xylene. Each component spectrum corresponds to an IVO calculation at the indicated site. The sum has taken into account appropriate stoichiometric factors. The linewidths used in generating the simulated spectra are indicated in the text.

Fig. 4 compares the calculated and higher-resolution experimental spectra in the region of the main C 1s $\rightarrow \pi^*$ peak. Table 3 reports the calculated results for *ortho*-, *meta*- and *para*-xylene. Fig. 5 presents an energy level diagram of the calculated excitations from the C 1s(C-R) and C 1s(C-H) levels to the $b_1(b_{3u})$ component of the $1\pi^*$ level, along with sketches of the $\pi^*b_1(b_{3u})$ MO in each of the localised core hole states. Note this figure only displays the transitions to the b_1 (or b_{3u}) state since the transitions to the $a_2(a_u)$ all have negligible intensity according to the calculation. In all three isomers the b_1 (or b_{3u} in *para*) component of the $1\pi^*$ level always lies below the $a_2(a_u)$ component, independent of the location of the core hole. Interestingly, the calculations predict quite significant shifts in the b_1 and a_2 binding energies as a function of core hole location. The constancy of the orbital ordering of the symmetry

split components of the $1\pi^*$ orbital is consistent with the ordering of the split π components found in the earlier valence charge transfer studies of the isomeric xylenes [5,6]. The calculated energies are 2 eV higher than the experimental energies. Aside from this, the overall intensity and the calculated shape of the main π^* band are in reasonable agreement with experiment, with splittings and asymmetries being reproduced, although not the relative intensities of components, nor the overall width. The discrepancy in both of the latter areas may be associated with the absence of any treatment of vibrational band structure in the calculation. Benzene has a strong vibrational band structure [22] with both C–C and C–H stretching modes being active. This vibrational band structure extends the electronic excitation to higher energy, as found experimentally.

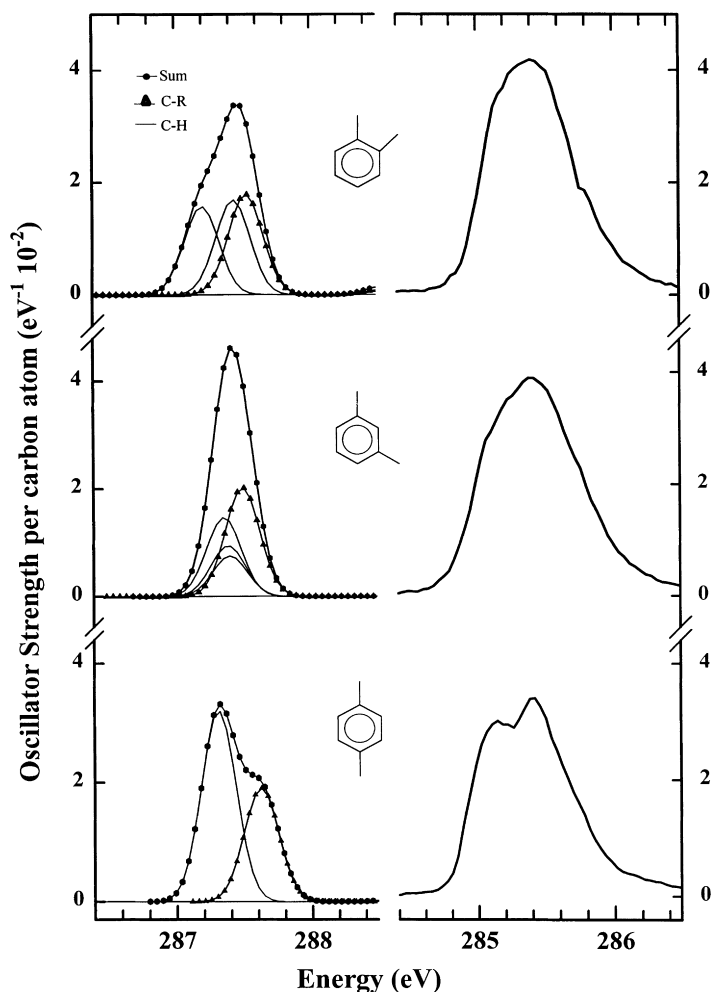


Fig. 4. Comparison of calculated and experimental spectra in the region of the main C 1s \rightarrow $1\pi^*$ band (for calculated signal: points = sum; triangles = C-R component; solid lines = C-H and Me components). The intensities and energies are reported on absolute scales for both experiment and calculation.

5. Discussion

As in the earlier studies of the dimethylphthalate [7] and nitroaniline isomers [8], we have found that the main π^* peak has two resolvable components in *para*-xylene but only one in *ortho*- and *meta*-xylene. What is the origin of this splitting, and can it be related to the spectral interpretation used to explain the splitting in *para*-dimethylphthalate? Since the calculations reproduce the essential aspects of the isomeric dependence of the shape of the main π^* peak, it is reasonable to turn to the details of these calculations as a basis for our answer to these questions.

Experimentally and computationally, there is no significant shift in the energy of the centroid of the main π^* peak in the spectra of *ortho*-, *meta*- and *para*-xylene. This is different from the dimethylphthalates, where there is a 0.47 eV shift in the $\pi^*_{\text{C=O}}$ and a 0.26 eV shift in the $\pi^*_{\text{C=C}}$ energy over the isomeric series [7]. The absence of such shifts in the xylene series is likely related to the absence of any strong electronegativity difference between the methyl substituent and the ring.

The calculations clearly indicate that the C 1s \rightarrow $1\pi^*$ transition is dominated by C 1s(C-H) and C 1s(C-R) excitation to the lower-energy b_1 component (b_{3u}

Table 3

Calculated IPs, term values and oscillator strengths for C 1s \rightarrow π^* transitions in *para*-, *meta*- and *ortho*-xylene

Carbon no.	Core hole position	Orbital character	IP (eV)	TV (eV)	Oscillator strength ^a ($\times 10^{-2}$) eV ⁻¹
<i>ortho</i> -xylene					
C ₁ , C ₂	C-R	$\pi^*(b_1)$	290.33	2.81	2.28 ($\times 2$)
		$\pi^*(a_2)$		1.78	0.11
C ₃ , C ₆	C-H	$\pi^*(b_1)$	290.28	3.09	2.00 ($\times 2$)
		$\pi^*(a_2)$		1.49	0.0000
C ₄ , C ₅	C-H	$\pi^*(b_1)$	290.33	2.90	2.15 ($\times 2$)
		$\pi^*(a_2)$		1.79	0.07
C ₇ , C ₁₁	Me	$\pi^*(b_1)$ /C-H	290.47	1.39	0.10 ($\times 2$)
		(2s)		1.09	0.25
		b ₁		0.74	0.0000
<i>meta</i> -xylene					
C ₁ , C ₃	C-R	$\pi^*(b_1)$	290.49	3.00	2.58 ($\times 2$)
		$\pi^*(a_2)$		1.73	0.0000
C ₂	C-H	$\pi^*(b_1)$	290.14	2.74	1.92 ($\times 1$)
		$\pi^*(a_2)$		1.70	0.0000
C ₄ , C ₆	C-H	$\pi^*(b_1)$	290.14	2.78	1.88 ($\times 2$)
		$\pi^*(a_2)$		1.70	0.0000
C ₅	C-H	$\pi^*(b_1)$	290.49	3.11	2.41 ($\times 1$)
		$\pi^*(a_2)$		1.70	0.0000
C ₇ , C ₁₁	Me	$\pi^*(b_1)$ /C-H	290.57	1.36	0.84 ($\times 2$)
<i>para</i> -xylene					
C ₁ , C ₄	C-R	b _{3u}	290.36	2.74	2.43 ($\times 2$)
		a _u		1.92	0.0000
C ₂ , ₃ , C ₅ , ₆	C-H	b _{3u}	290.30	2.99	2.04 ($\times 4$)
		a _u		1.61	0.05
C ₇ , C ₁₁	Me	$\pi^*(b_{3u})$ /C-H	290.55	1.22	0.17 ($\times 2$)

^aCalculated C 1 π^* oscillator strength per transition. The experimental C 1 π^* oscillator strength ($\times 10^{-2}$) per carbon atom, averaged over all the C 1s \rightarrow 1 π^* signal determined from the low-resolution/high-resolution spectra is 2.4/3.3 (*ortho*-xylene), 2.3/2.6 (*meta*-xylene), 2.5/2.7 (*para*-xylene).

in *para*), with negligible contribution from excitation to the a₂(a_u) component. The calculation also indicates that the origin of the split π^* peak in *para*-xylene is associated with a displacement of the C 1s \rightarrow $\pi^*(b_{3u})$ transition at the methyl-substituted ring carbons relative to the corresponding transition at the unsubstituted C 1s(C-H) carbons. This ~ 0.3 eV shift arises partly from the conventional C-H to C-R core level shift (+0.06 eV), but mostly from the change in the binding energy of the $\pi^*(b_{3u})$ level when the core hole is moved from the C-H to the C-R carbon (IP(C-R) – \langle IP(C-H) \rangle = +0.25 eV). In *meta*-xylene the energy of the corresponding $\pi^*(b_1)$ level also changes as the core hole is shifted from the C-H to the C-R carbon (–0.15 eV), but this shift is largely compensated by a complementary shift (+0.25 eV) in the C 1s IP, leaving a net shift of only +0.1 eV. In

combination with the spread in the C 1s(C-H) \rightarrow $\pi^*(b_1)$ transition over the four different C-H environments in *meta*-xylene, the net effect is a nearly symmetric overall lineshape. In *ortho*-xylene the calculated C 1s IP is essential independent of core hole location (IP(C-R) – \langle IP(C-H) \rangle = +0.02 eV). However, according to the calculation, the binding energy of the $\pi^*(b_1)$ orbital changes by +0.19 eV (on average) as the core hole is shifted from the C-H to the C-R carbon. Fig. 5 depicts all of these shifts on a to-scale energy level diagram, clearly showing the roles of changes in core-binding energy and core hole-induced π^* energies in determining the detailed π^* lineshapes in each species.

From the ab initio calculations we conclude that the splitting of the main π^* peak clearly observed experimentally in the *para*-isomer is a result of changes in

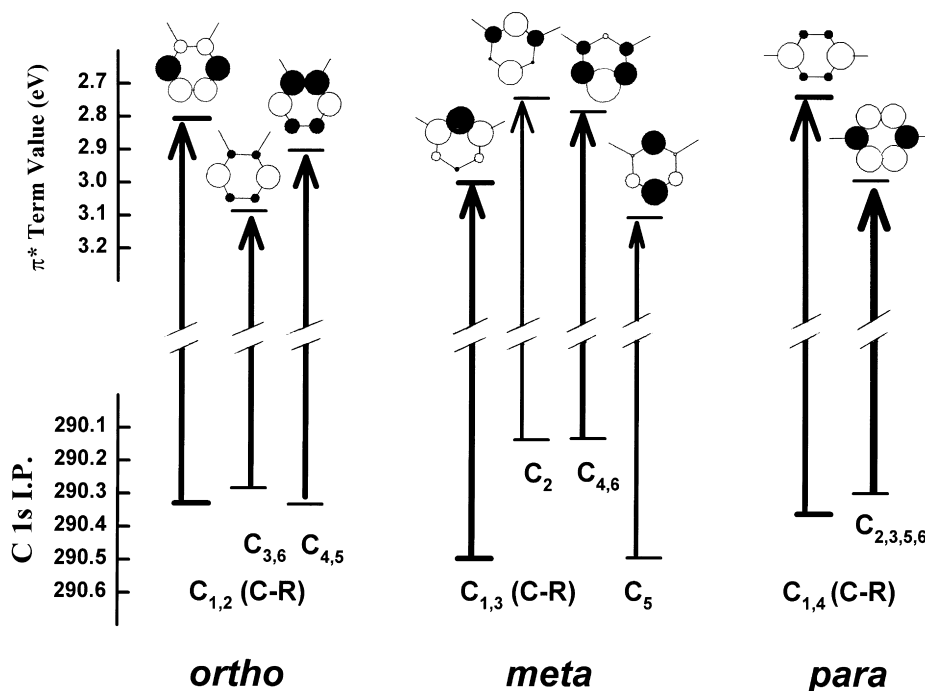


Fig. 5. Schematic of the calculated components of the C 1s(C-R) \rightarrow $1\pi^*(b_1)$ and C 1s(C-H) \rightarrow $1\pi^*(b_1)$ transitions. C 1s(C-R) excitation and C 1s(C-H) excitation at all sites are indicated, with spacings proportional to the computed IPs and level binding energies (see Table 3). Molecular orbital pictures derived from the results of the GSCF3 calculation are indicated. Appropriate linear combinations were used to regenerate the true molecular symmetry from the localised core hole results.

the energy of the $\pi^*(b_{3u})$ level as the core hole is shifted from the C-H to the C-R site. The splitting could be described as a ‘C-R’ effect, although as noted above, most of the shift in the excitation energy is related to site dependence of the π^* energy, not shifts in the C 1s level. Thus, it is not a direct chemical shift of the C 1s(C-R) energy, but rather an indirect effect, presumably related to different degrees of core hole relaxation at the two sites. The *ab initio* calculations predict systematic variations in the energy of the C 1s(C-R) \rightarrow $1\pi^*$ transition with isomeric form and predict a more prominent splitting in *para*- than in *ortho*- or *meta*-xylene, as found experimentally.

This result, both experimental and theoretical, is quite different from that found in the dimethylphthalates [7]. In that case, as in the nitroanilines [8], the C 1s(C-R) chemical shift is very large (> 1 eV) so that the C 1s(C-R) transitions occur elsewhere, in a completely separate band. The splitting in the π^* peak in the 1,4-DMP (*para*-) species is related to a particu-

larly large intensity of the C 1s \rightarrow $\pi^*(a_2)$ transition. According to the calculations for the xylenes there is negligible intensity for C 1s \rightarrow $\pi^*(a_2)$ transitions at any site in any isomer. In the isomeric nitroanilines [8], where a splitting was found in the $1\pi^*$ band of *para*-nitroaniline, the lower energy peak was assigned to C 1s(C-H) \rightarrow $\pi^*(6b_1)$ transitions and the higher-energy peak to C 1s(C-H) \rightarrow $\pi^*(7b_1)$ transitions.

The experimental component of this work, combined with that of the earlier studies [7,8] indicates that C 1s spectroscopy can be an effective tool to identify *para*-substitution through observation (at sufficiently high energy resolution) of a broader and/or split main π^* peak, relative to *ortho*- and *meta*-substitution patterns of the same substituents. However, our studies also indicate that the origin of this splitting can be quite subtle and likely will differ from species to species. The combined set of three studies indicates that the *para*-isomer is always ‘odd man out’ but that the reason is system-dependent—likely ‘C-R’ related

in the xylenes, a_2/b_2 isomeric selectivity in dimethylphthalates [7], and a very complex interplay of delocalization and chemical shift in the nitro-anilines [8].

Acknowledgements

This work has been supported by the Natural Sciences and Engineering Research Council of Canada. We thank Dr. N. Kosugi for providing his GSCF3 code and assisting us with its operation.

References

- [1] E. Yamamoto, T. Yoshidome, T. Ogawa, H. Kawazumi, *J. Electron Spectroscopy Relat. Phenom.* 63 (1993) 341.
- [2] Y. Kanada, R. Shimada, *Spectrochim. Acta* 17 (1961) 279.
- [3] A. Bolovinos, J. Philis, E. Pantos, P. Tsekeris, G. Andritso-poulos, *J. Mol. Spectrosc.* 94 (1982) 55.
- [4] K. Kesper, N. Münzel, W. Pietzuch, H. Specht, A. Schweig, *J. Mol. Structure (Theochem.)* 200 (1989) 375.
- [5] B. Uno, Y. Ninomiya, K. Kano, T. Kubota, *Spectrochim. Acta* 43A (1987) 955.
- [6] T. Kubota, Y. Matsuhisa, K. Kano, Y. Ninomiya, *Mol. Cryst. Liq. Cryst.* 126 (1985) 111.
- [7] S.G. Urquhart, A.P. Hitchcock, A.P. Smith, H. Ade, E.G. Righthor, *J. Phys. Chem. B* 101 (1997) 2267.
- [8] C.C. Turci, S.G. Urquhart, A.P. Hitchcock, *Can. J. Chem.* 74 (1996) 851.
- [9] N. Kosugi, *Theor. Chim. Acta* 72 (1987) 149.
- [10] N. Kosugi, H. Kuroda, *Chem. Phys. Lett.* 74 (1980) 490.
- [11] A.P. Hitchcock, *Physica Scripta* T31 (1990) 159.
- [12] A.P. Hitchcock, D. Mancini, *J. Electron Spectrosc.* 67 (1994) 1.
- [13] S. Huzinaga, J. Andzelm, M. Klobokowski, E. Radzio-Andzelm, Y. Sasaki, H. Tatewaki, *Gaussian Basis Sets for Molecular Calculations*, Elsevier, Amsterdam, 1984.
- [14] W.J. Hunt, W.A. Goddard III, *Chem. Phys. Lett.* 3 (1969) 414.
- [15] N. Kosugi, E. Shigemasa, A. Yagishita, *Chem. Phys. Lett.* 190 (1992) 481.
- [16] N. Kosugi, J. Adachi, E. Shigemasa, A. Yagishita, *J. Chem. Phys.* 97 (1992) 8842.
- [17] Spartan version 4.0, Wavefunction Inc., 18401 Von Karman Ave., #370, Irvine, CA 92715.
- [18] K. Kuchitsu (Ed.) *Structure Data of Free Polyatomic Molecules*, vol. 7, Landolt-Bornstein, New Series II, Springer, Berlin, 1976.
- [19] J.A. Horsley, J. Stohr, A.P. Hitchcock, D.C. Newbury, A.L. Johnson, F. Sette, *J. Chem. Phys.* 83 (1985) 6099.
- [20] I. Ishii, R. McLaren, A.P. Hitchcock, K.D. Jordan, H. Choi, M.B. Robin, *Can. J. Chem.* 66 (1988) 2104.
- [21] W.L. Jolly, K.D. Bomben, C.J. Eyermann, *At. Data Nucl. DataTables* 31 (1984) 109.
- [22] Y. Ma, F. Sette, G. Meigs, S. Modesti, C.T. Chen, *Phys. Rev. Lett.* 63 (1989) 2044.